Evaluating the Efficacy of Thrombolytic Agents on Dissolving Different Clot Structures

Saleheh Heydari Ghasemi[1], Mohammad-Taghi Ahmadian[*], Ahmad Assempour[1]

[1]School of Mechanical Engineering, Sharif University of Technology, Tehran, Iran

Abstract

Thrombolytic therapy is an effective method for dissolving blood clots that block cerebral arteries and cause strokes. Through this procedure, plasminogen activators are used to recanalize vessels and restore blood flow. This study investigates the dissolution of clots with different structures using three plasminogen activator drugs. Fibrin clots with coarse and fine fibrin fibers, as well as retracted clots representing aged clots with reduced serum, are analyzed. The dissolution model includes the dynamics of flow within the vessel and clot, the elasticity of the vessel wall, and its interaction with the fluid. Drug transport into the clot is modeled by convection and diffusion. The results indicate that treatment regimens with alteplase, reteplase, and tenecteplase are safe and effective in dissolving clots across all structures considered. However, lysis activation time and vessel recanalization time are significantly shorter with tenecteplase and alteplase compared to reteplase. Additionally, coarse clots with larger fibrin fibers dissolve faster than fine clots, and retracted clots require nearly twice as much time to dissolve.

Keywords: Thrombolytic therapy; Alteplase; Reteplase; Tenecteplase; Fiber radius; Retracted clots; Finite element analysis

1. Introduction

Acute ischemic stroke (AIS), the most common form of stroke and the third major cause of mortality globally [1], occurs when a thrombus blocks blood flow in a cerebral vessel, leading to an inadequate blood supply to brain cells. To prevent cell necrosis, immediate medical intervention is essential. One promising treatment procedure is thrombolytic therapy, which involves the use of thrombolytic agents such as tissue plasminogen activator (tPA) to dissolve blood clots. This procedure can help limit stroke damage and improve the chances of recovery, although it poses a significant risk of serious hemorrhagic complications. The effectiveness of thrombolysis relies on multiple factors, including the characteristics of the clot, the drug used, and the general health of the patient. Ongoing research is focused on developing therapeutic approaches to increase lysis rates.

The lytic rates of clots are influenced by their properties, such as fiber diameter [2] and degree of retraction [3, 4]. The environment in which a fibrin clot forms determines its structure. High ionic concentrations result in fine clots with thin, densely packed fibers and small pores, whereas low ionic concentrations produce coarser clots with thicker fibers and larger pores [5]. Some experiments demonstrate that coarse clots with thick fibers lyse faster than fine clots with thin

[*] Corresponding author at: School of Mechanical Engineering, Sharif University of Technology, Tehran, Iran.
Tel.: +982166165503; fax: +982166000021
E-mail address: ahmadian@sharif.edu

fibers [6, 7], even though thick fibers lyse slower individually [8]. Conversely, other experiments indicate that fine clots lyse quicker or exhibit no notable difference in the lysis rate [9, 10].

Clot retraction significantly alters the internal structure and composition of the clot by expelling its serum [11], which results in decreased permeability and fluid phase volume [12]. Retracted clots, which are significantly more resistant to thrombolysis than non-retracted clots [13], are utilized to replicate the thrombolysis of aged thrombi. Their reduced susceptibility to thrombolysis may be attributed to the decreased fluid phase plasminogen (PLG) within the clot [14]. Also, the transport properties of thrombolytic drugs in a retracted clot are mainly influenced by the decreased permeability of the fibrin structure.

The type of thrombolytic agent used is another crucial factor impacting the effectiveness of thrombolytic therapy. Different agents differ in stability, half-life, and fibrin specificity. The initial generation of thrombolytic agents, streptokinase and urokinase, are not specific to fibrin and bind rapidly to PLG in both plasma and clots [15]. This can cause excessive PLG depletion and an increased risk of intracranial hemorrhage (ICH) [16]. Clinical trials of streptokinase and urokinase revealed a high mortality rate and no significant enhancement in recanalization [17, 18]. Second-generation agents, including tPA and pro-urokinase, are fibrin-specific and show a low affinity for PLG in the absence of fibrin [15]. This targeted approach allows for localized fibrinolysis on the surface of the clot, reducing systemic effects and the risk of ICH [16]. Alteplase, a tPA variant, is the only thrombolytic agent with FDA approval in AIS treatment. However, further studies suggest that the effectiveness of alteplase is limited by plasminogen activator inhibitor-1 (PAI-1), its short half-life, and an increased risk of ICH. Modified tPA variants, such as reteplase and tenecteplase, have been designed to enhance specific characteristics, such as a longer half-life, fewer side effects, and greater resistance to inhibition, making them promising therapeutic options [19-22]. Reteplase has a longer half-life and lower affinity for fibrin. This decreased binding affinity allows unbound reteplase to penetrate more effectively, potentially improving its fibrinolytic activity. Tenecteplase, another modified tPA variant, offers a longer half-life, improved fibrin specificity, and greater resistance to PAI-1. Despite promising theoretical advantages, no tPA variants have outperformed alteplase in clinical outcomes for AIS treatment [20-23]. Recently, clinical studies reported similar effectiveness and ICH risk between these variants and alteplase [20]. These clinical outcomes do not fully support the theoretical advantages. Hence, it is essential to evaluate the effectiveness and safety of these thrombolytic agents systematically.

The administration of tPA leads to complex chemical reactions within the vasculature by activating PLG and generating plasmin (PLS), which degrades fibrin fibers. Comprehending the interactions among the involved components is essential to elucidate the mechanisms of fibrinolysis and to develop therapeutic strategies. Considering the limited clinical data available because of the narrow intervention window and safety concerns of experimental studies, utilizing computational modeling techniques offers a valuable tool for better understanding the mechanisms of thrombolysis. Mathematical models can effectively simulate the impact of thrombolytic therapy on blood flow and tPA transportation into clots and can predict the risk of ICH.

Considerable work has been done on thrombolysis modeling [5, 9, 24-29]. One of the pioneering models of fibrinolysis was presented by Diamond and Anand [9], who solved a set of convection-

diffusion-reaction equations to describe the concentration of thrombolytic agents. In their model, the clot was treated as a porous medium with a uniform fibrin network. However, their model incorrectly represents clot dissolution as a reduction in fiber diameter rather than the transverse cutting of fibrin fibers. Piebalgs et al. [24] proposed a model consisting of a 3D thrombolysis model and a compartmental model to capture protein concentration variations in plasma. Later, their model was further extended by Gu et al [25] to account for the delayed clearance of tPA during the drug distribution process. Their model treats the vessel wall as rigid, which leads to an overestimation of blood flow velocity during the lysis process. Ghasemi [26] found that for precise modeling of clot dissolution, the impact of arterial walls must be considered, because rigid models do not correctly estimate the time needed for clot dissolution. While numerous attempts have been made to model the complex process of clot dissolution, the specific effects of different tPA variants, such as reteplase and tenecteplase, on clots with distinct fibrin structures remain insufficiently explored. Also, the lysis of retracted clots using computational models that account for arterial flow dynamics, vessel wall interactions, and the convective-diffusive transport of the drug has not been investigated.

This study aims to investigate the dissolution of three different clot structures to evaluate the safety and efficacy of three drugs, namely, alteplase, reteplase, and tenecteplase. This objective will be accomplished by analyzing the hemodynamics of flow within the vessel and clot, along with the transport of drugs to and within the clot via diffusion and convection. Additionally, the impact of vessel wall elasticity will be examined using the two-way coupled fluid-structure interaction (FSI) technique, which allows for a detailed assessment of the mechanical behavior of the vessel wall in response to hemodynamic forces. This comprehensive approach aims to enhance our understanding of the interplay between fluid flow, clot structure, and drug efficacy, ultimately contributing to the development of more effective and safer thrombolytic therapies.

2. Method

2.1. Geometry

A two-dimensional model of the internal carotid artery (ICA) bifurcating into the middle cerebral artery (MCA) and anterior cerebral artery (ACA) is constructed, as shown in Figure 1, and a 3-mm fibrin clot is placed at the beginning of the MCA in an 80 kg individual, causing complete occlusion. This location is one of the areas with a high likelihood of clot formation. The vessel length is 11.6 mm, with diameters of 2.9 mm, 2.3 mm, and 1.7 mm for the ICA, MCA, and ACA, respectively. The wall thicknesses are 0.45 mm for the ICA, 0.4 mm for the MCA, and 0.32 mm for the ACA [30].

2.2. Dynamics of the blood flow

Blood is modeled as an incompressible Newtonian fluid, and the flow is presumed to be laminar. Blood flow within the free region of the vessel is governed by the Navier-Stokes equation. The clot domain is modeled as a porous media, and for the governing equation of the flow through it, the Brinkman equation [31] is applied as

$$\frac{1}{\varepsilon}\rho_f \frac{\partial \mathbf{v}_f}{\partial t} + \frac{1}{\varepsilon}\rho_f (\mathbf{v}_f \cdot \nabla)\mathbf{v}_f \frac{1}{\varepsilon} = \nabla \cdot [-pI + \mathbf{K}] - (\mu k^{-1})\mathbf{v}_f \tag{1}$$

$$\mathbf{K} = \mu \frac{1}{\varepsilon}(\nabla \mathbf{v}_f + (\nabla \mathbf{v}_f)^T),$$

In equation (1), $\mathbf{v}_f$ is the blood velocity, p is the blood pressure, and I is the identity matrix. Furthermore, the fluid density ρ_f and blood dynamic viscosity μ are assumed to be 1050 kg/m^3 and 0.0037 Pa·s, respectively. The clot parameters ε and k are the clot porosity and permeability. To apply boundary condition, a steady flow rate of 4.31 mL/s, based on the average pulsatile ICA flowrate reported in the literature [32], is specified at the inlet. At both outlets, physiological pressure is defined using a 3-element Windkessel model [33] described as

$$Q(t)(1 + \frac{R_1}{R_2}) + CR_1 \frac{dQ}{dt} = C\frac{dP}{dt} + \frac{P}{R_2}. \tag{2}$$

The parameters of the Windkessel model are obtained from the literature [34]. It should be noted that, in both Navier-Stokes and Brinkman equations, the same pressure and velocity fields are applied. This ensures continuous pressure at the interface between the free-flow and porous regions and maintains the continuity between the fluid velocity in the free-flow domain and the Darcy velocity in the porous domain.

2.3. Dynamics of the artery

Blood flow exerts force on the flexible wall of the artery, resulting in wall deformation. The dynamics of the artery wall is described as:

$$\rho_s \frac{\partial^2 \mathbf{u}_s}{\partial t^2} = \nabla \cdot S + F \tag{3}$$

where $\mathbf{u}_s$ is the artery displacement, S represents the second Piola–Kirchhoff stress, and F denotes the total force exerted by fluid on the vessel. ρ_s is the density of the artery set to be 1050 kg/m^3, given that the densities of the wall and the blood are nearly identical. The entrance and outlets of the artery wall are considered to be fixed, and the no-slip condition is applied at the interface with the blood. The vessel wall is considered as linear elastic material in the model, with a Young's modulus of 1.5 MPa and a Poisson's ratio of 0.45.

To model the interaction between the blood flow and artery wall, the force on the inner boundary of the artery and its wall displacement rate are calculated. Since the fluid flow and solid wall equations are expressed in spatial and material reference frames, respectively, the arbitrary Lagrangian-Eulerian (ALE) method is used to describe their interaction at the interface.

2.4. Concentration changes of fibrinolytic proteins

2.4.1. Drug administration regimens

Alteplase exhibits a high affinity for fibrin and PLG. However, it is characterized by a notably short half-life of approximately 5 minutes. The standard dosing regimen for alteplase is 0.9 mg/kg, with %10 of the total dose administered as an initial intravenous (IV) bolus over 1 minute, followed by the infusion of the remaining %90 over the subsequent 60 minutes. Reteplase demonstrates a greater ability to diffuse through clots compared with alteplase. This agent has a lower affinity for PLG but benefits from a longer half-life. The recommended dosing regimen for reteplase involves double bolus administration, with each bolus consisting of 17.4 mg given over 2 minutes, separated by a 30-minute interval [21]. Tenecteplase offers several advantages over its predecessor. It has higher fibrin specificity, an extended half-life, and increased resistance to PAI-1. Tenecteplase is administered at a dosage of 0.25 mg/kg, not exceeding a total of 25 mg, delivered as a single IV bolus within 5 seconds [20].

2.4.2. Concentration changes of fibrinolytic proteins in plasma

The administration of tPA initiates a chain of reactions within the plasma. tPA interacts with PLG to generate PLS. Similarly, urokinase plasminogen activator (uPA), present in low concentrations in plasma, also activates PLG to produce PLS. PLS then interacts with fibrinogen (FBG), resulting in the formation of fibrin degradation products (FDP). The activity of PLS is regulated by two inhibitors, α_2-antiplasmin (AP) and α_2-macroglobulin (MG). Additionally, tPA and uPA are inhibited by PAI-1. These plasma reactions are listed in Table 1.

Variations in the concentrations of these factors, driven by the reactions and their transport through blood plasma, play a crucial role in the clot dissolution process and the treatment outcomes. The convection-diffusion-reaction equation is used to represent the temporal and spatial changes in concentrations as

$$\frac{\partial c_i}{\partial t} = \nabla \cdot (D_i \nabla c_i) - \mathbf{v}_f \cdot \nabla c_i + R_i \tag{4}$$

In the above equation, c_i represents the concentration of fibrinolytic factors in plasma, $\mathbf{v}_f$ represents the fluid velocity obtained from the Navier-stokes equation, D_i is the diffusion coefficient, and R_i is the concentration changes due to performed reactions mentioned in Table 1.

2.4.3. Concentration changes of fibrinolytic proteins in clot

Drug administration increases its concentration in the bloodstream, resulting in significant adherence to the binding sites on the clot surface. It interacts with bound-phase PLG to produce PLS, which degrades fibrin fibers in the clot, leading to clot dissolution. Additionally, the drug, PLG, and PLS are able to detach from the clot and enter the plasma or conversely attach from the plasma phase to the clot. The changes in concentrations of these factors in the clot phase are detailed by

$$\frac{\partial (\varepsilon c_i)}{\partial t} = \nabla \cdot (D_i \nabla c_i) - \mathbf{v}_f \cdot \nabla c_i + \varepsilon R_i. \tag{5}$$

The reactions in the fluid phase of the clot are identical to those in the plasma. The reactions in the pore phase are mentioned in Table 2.

To implement the boundary condition in the convection-diffusion-reaction equation, the concentration constraint at the inlet is applied using a method developed by Gu et al [25]. This method tracks temporal changes in species concentration within the bloodstream. It employs a two-compartment model, namely central and peripheral compartments, to depict the effect of tPA injection on the concentration of other fibrinolytic proteins. The central compartment, representing plasma, includes tPA, uPA, and other proteins. tPA is administered here, and both tPA and uPA can migrate between the compartments. The transport of other proteins between compartments is treated as negligible. The two-compartment model takes into account the delayed clearance of tPA and uPA during drug distribution. The temporal changes of tPA and uPA concentration in the central and peripheral compartments are described as

$$\frac{dc_{c,PA}}{dt} = -k_{el,PA}c_{c,PA} - k_{cp,PA}c_{c,PA} + k_{pc,PA}c_{p,PA} + R_{PA} + S_{PA} + \frac{I}{V_c M_{w,PA}} \tag{6}$$

$$\frac{dc_{p,PA}}{dt} = k_{cp,PA}c_{c,PA} - k_{pc,PA}c_{p,PA} \tag{7}$$

The plasma concentration of other fibrinolytic proteins can be represented as:

$$\frac{dc_{i,sys}}{dt} = -k_{el,i}c_{i,sys} + R_i + S_i \quad i = PLG, PLS, AP, FBG, MG, and\ PAI - 1 \tag{8}$$

In equations (6) and (8), k_{el} represents the elimination constant, accounting for the reduction in plasma concentration of species due to their half-life. R_i denotes the plasma reactions mentioned in Table 1, and S_i signifies the rate of systematic generation of species. The values of k_{el} and S_i for each component can be determined from their half-life and initial concentration in blood plasma [24]. The term $\frac{I}{V_C M_{W,PA}}$ indicates the increase in PA concentration within plasma due to infusion, where I, V_C, and $M_{W,PA}$ are the infusion rate, the volume of plasma in the circulatory system, and the molecular weight of PA, respectively. As there is no uPA injection, this term is zero and is not applicable for uPA. In equation (7), the constants $k_{cp,PA}$ and $k_{pc,PA}$ represent the rates at which PA moves between the two compartments. Equations (6)-(8) are solved using the 4th order Runge-Kutta method for the complete duration of drug administration before the simulation. The resulting concentrations are utilized as inlet boundary condition for the convection-diffusion-reaction equation.

2.5. Lysis equations

This study employs the dissolution model proposed by Piebalgs et al [24]. This model examines the progression of clot dissolution by analyzing the total number of binding sites and the occupancy

of these sites by PLG, PLS, and tPA. The parameter EL is defined based on the concentration of total binding sites relative to the initial binding sites, indicating the progression of clot dissolution. This parameter is calculated as follows

$$E_L = 1 - \frac{n_{tot}}{n_{tot,0}}. \tag{9}$$

Changes in the concentration of binding sites over time are described by the concentration of bound-phase PLS, n_{PLS}, as

$$\frac{\partial n_{tot}}{\partial t} = -k_{deg}\gamma n_{PLS} \tag{10}$$

The concentration of bound-phase PLS, PLG, and tPA is also determined by

$$\frac{\partial n_i}{\partial t} = R_i^{clot},\ i = tPA.fibrin, PLG.fibrin, and\ PLS.fibrin, \tag{11}$$

where R_i^{clot} is the reactions in the pore phase of the clot and mentioned in The reactions in the fluid phase of the clot are identical to those in the plasma. The reactions in the pore phase are mentioned in Table *2*.

. E_L is a parameter that indicates the progress of clot lysis. To reduce the computational cost, when E_L reaches 0.95, the clot is assumed to be dissolved in that area, and flow is considered restored. If E_L is lower than this threshold in non-retracted clots, the permeability is calculated using Davis's equation [43] as

$$k(\varepsilon, R_f) = \frac{4R_f^2}{70(1-\varepsilon)^{1.5}[1+52(1-\varepsilon)^{1.5}]} \tag{12}$$

For retracted clots, permeability also depends on the degree of clot retraction and the blood hematocrit level. By considering the volume of serum exuded during retraction, a compaction parameter can be defined as:

$$C = (R^G - (H + (1-H)\alpha)) / ((1-H)(1-\alpha)) \tag{13}$$

where R^G and H are the retraction and hematocrit levels assumed to be 0.5 and 0.4 for %50 retraction, respectively [44]. α denotes the density ratio of FBG in plasma relative to that in fibrin fibers. The permeability of the retracted blood clot [44] is obtained as:

$$k_{retracted} = k(\varepsilon, R_f) \cdot \frac{(1-H)\alpha + C(1-H)(1-\alpha)}{H + (1-H)\alpha + C(1-H)(1-\alpha)} \tag{14}$$

If E_L exceeds the threshold, the permeability of the clot is considered to be infinite. Throughout the dissolution process, clot porosity varies continuously and is calculated as follows:

$$\varepsilon_{clot} = 1 - \varphi_0 (1 - E_L) . \quad (15)$$

Depending on its composition, the porosity of the clot ranges from 0.75 to 0.99 [44]. In this study, φ_0 is chosen to be 0.1, resulting in a porosity of 0.9.

2.6. Simulation details

A computational mesh with 7087 triangular elements is generated. The finite element method is employed to solve the fully coupled differential equations of fluid flow, vessel wall mechanics, species transport, and clot lysis. The Newton method is applied with the Parallel Space Direct Solver (PARDISO) [45], and the Backward Differentiation Formula (BDF) automatically selects the time steps. The simulation time is 3700 seconds, enough to complete the clot lysis and restore flow in all cases, with results saved every second. Each simulation took approximately 10 hours on an Intel Core i7-4790K processor with 16.0 GB RAM. Additionally, a grid independence study is conducted, refining the mesh to 15126 elements. Results show an approximate 8-second difference in lysis completion time between meshes of 7087 and 15126.

3. Results

This study evaluates the lysis of various clot structures using three drugs, namely, alteplase, reteplase, and tenecteplase. Clots are classified as either non-retracted or retracted to assess the dissolution of aged clots. Retracted clots are assumed to be %50 retracted, which means approximately %84.2 of their original plasma volume as serum is exuded. Moreover, to study the effect of fibrin fiber radius, two radii of 60 and 100 nm representing fine and coarse clots in non-retracted clots are examined. Table 3 presents the drug, clot type, and fibrin radius for each simulation.

3.1. Concentration of species in blood plasma

The administration of tPA alters the concentrations of fibrinolytic factors involved in the clot dissolution process in the circulatory system, as depicted in Figure 2. Figure 2a shows an increase in the concentration of the drug after injection in all variants of tPA. Specifically, following the initial one-minute injection of alteplase, its concentration in the blood increases dramatically. A one-minute delay before starting continuous infusion leads to a sudden drop in concentration. Continuous infusion then causes a gradual increase, persisting until the end of the continuous injection. Reteplase, administered in two steps 30 minutes apart, achieves peak concentration twice: initially in the first two minutes and again 30 minutes later with the second dose. For the remainder of the simulation, reteplase levels decrease due to PAI-1 activity and its half-life. Tenecteplase, administered as a 5-second bolus, rapidly reaches peak concentration post-injection and then gradually declines until the end of the simulation. As illustrated in Figure 2b, the initial concentration of uPA in blood plasma drops significantly due to its strong affinity for reacting with PAI-1. However, as PAI-1 levels decrease following tPA injection, uPA concentration gradually rises, maintaining this gradual increase until the end of the simulation. As shown in Figure 2c,

after tPA injection, the interaction between this drug and PLG in blood plasma leads to a reduction in PLG concentration. Alteplase causes the most decrease, reducing PLG level to %36 of its normal value by the end of the administration. Reteplase also reduces PLG concentration, but the reduction is minimal. Tenecteplase decreases PLG level, with concentrations reaching approximately %77 of the initial value after 3700 seconds. The changes in FBG and AP levels follow a similar pattern to PLG, as shown in Figure 2d and Figure 2e, respectively. During alteplase administration, there is a more pronounced decrease in both FBG and AP. In contrast, these blood factors remain nearly unchanged after reteplase injection. Figure 2f shows that the changes in MG concentration across all drug regimens are minimal because MG is a weaker inhibitor of PLS compared with AP, which is the primary inhibitor. These changes are more pronounced with alteplase administration and least noticeable with reteplase. The administration of drugs and their increasing concentration in plasma lead to a more substantial reaction with PAI-1, causing a sharp decrease in PAI-1 concentration within minutes, as shown in Figure 2e. This decrease is most significant with alteplase. Conversely, Tenecteplase administration results in a slower rate of PAI-1 decrease, maintaining higher PAI-1 levels until the end of the simulation. PLS concentration changes are minimal due to its rapid inhibition in blood plasma by AP and MG. The extent of the changes is greater with alteplase and lesser with reteplase injection.

3.2. Lysis activation time

Drug administration and its interaction with PLG in the clot lead to the degradation of fibrin, which increases clot porosity. As this process progresses, the clot begins to dissolve and decrease in size. For coarse clots with a fibrin fiber radius of 100 nm, dissolution starts at 358, 2473, and 447 seconds after injecting alteplase, reteplase, and tenecteplase, respectively. In fine clots, the corresponding times are 386, 2469, and 413 seconds, respectively. For retracted clots, dissolution starts at 382, 2467, and 459 seconds. These findings indicate that lysis activation time depends on the drug type rather than clot structure. Reteplase initiates lysis much later than the other two drugs, while alteplase and tenecteplase have approximately similar activation times. Lysis activation time is affected by drug concentration in the plasma, fibrin affinity, and reaction activity of the drug [27].

3.3. Clot porosity

Figure 3 illustrates the average changes in porosity for coarse, fine, and retracted clots following the administration of the three drugs. Drug injection leads to an almost linear increase in clot porosity, continuing until the final stages of dissolution. As dissolution nears final stages, the rate of porosity increase slows, particularly with tenecteplase. This decrease may be attributed to the vessel recanalization and the reduced pressure gradient essential for flow. Furthermore, the obtained data indicate that the porosity increase rates for alteplase and tenecteplase are nearly identical and exceed that of reteplase. The figures also reveal that coarse clots with a 100 nm fibrin fiber radius dissolve more quickly than the other types, whereas fine clots require more time. Retracted clots dissolve more slowly due to their reduced permeability from serum exudation.

3.4. Recanalization time

Figure 4 illustrates the recanalization times for various drugs and clot structures. Recanalization occurs between 10 and 60 minutes post-drug injection. The quickest dissolution is observed with coarse clots treated with alteplase, primarily due to its high dosage. However, higher dosages also elevate bleeding risk, highlighting a trade-off between dissolution rate and safety. Tenecteplase, with its unique design, achieves recanalization slightly slower than alteplase but at a much lower dose, demonstrating its high efficacy. Conversely, reteplase requires significantly more time for recanalization. For fine clots, dissolution takes 1.5 times longer with alteplase, 1.1 times longer with reteplase, and 1.6 times longer with tenecteplase compared to coarse clots. In retracted clots, these ratios are 2.2, 1.3, and 2 times, respectively, for alteplase, reteplase, and tenecteplase.

4. Discussion

This study examines the dissolution of coarse, fine, and retracted clots, which causes complete occlusion of the MCA, using three thrombolytic agents: alteplase, reteplase, and tenecteplase. Alteplase, a plasminogen activator, dissolves clots by converting PLG to PLS at the clot surface, but its efficacy is limited by a short half-life and interaction with PAI-1. Reteplase, with a longer half-life and slower plasma clearance than alteplase, has a lower affinity for fibrin, which might allow it to penetrate deeper into clots due to its higher diffusion coefficient. Tenecteplase, also possessing a longer half-life than alteplase, offers higher fibrin specificity [20], and reduced reaction with PAI-1. The administration of these drugs in blood plasma alters the concentration of blood factors, as illustrated in Figure 2. The total injection doses of alteplase, reteplase, and tenecteplase are 72 mg, 34.8 mg, and 20 mg, respectively. The area under the concentration-time curve reflects drug exposure. Notably, tenecteplase, despite being administered in a smaller dose compared to the other drugs, exhibited higher drug exposure and greater efficacy. In contrast, reteplase, administered at a higher dose than tenecteplase, showed lower drug exposure, potentially compromising treatment success. Alteplase demonstrated higher drug exposure than reteplase, which is due to its higher injection dose.

As shown in Figure 2d, following drug injection, FBG levels in blood plasma decrease, with final values after 3,700 seconds being %30, %95, and %78 of the initial levels for alteplase, reteplase, and tenecteplase, respectively. Low FBG concentrations in plasma increase the ICH risk, with levels below 3 μM considered a threshold for heightened bleeding risk [46]. In all drug regimens studied, the final FBG concentration remains above this threshold, confirming their safety. However, the administration of tenecteplase and reteplase at lower doses is associated with a smaller decrease in FBG levels, implying a reduced bleeding risk.

The concentration of PAI-1 is depicted in Figure 2g. A higher concentration of PAI-1 indicates that the drug exhibits greater resistance to inhibition by PAI-1. Thus, in alignment with previous theoretical studies [27], it is evident that tenecteplase is more resistant to inhibition by PAI-1 compared with alteplase and reteplase.

In the results section, lysis activation time is addressed, indicating that this time is dependent on the type of drug used rather than the clot structure. The activation time for dissolution using reteplase is significantly longer than that for the other two drugs, while alteplase and tenecteplase exhibit approximately similar activation times. These findings align with those of Yang et al., who also reported a longer activation time for reteplase [27].

Longer activation times correspond to longer recanalization times. Previous studies using transcranial Doppler have categorized recanalization time into three types: sudden (occurring in less than one minute), stepwise (occurring between 1 and 30 minutes post-injection), and slow (occurring in more than 30 minutes), with the average time of 23±16 minutes [47]. Christo et al. reported that %25 of patients treated with alteplase achieved complete or partial recanalization within 30 minutes [48]. The recanalization times observed in this study for alteplase align with these experimental findings. However, for the three clot structures examined, the retracted clots, which have longer recanalization times, showed dissolution times more consistent with experimental research results. This is due to the gradual formation and growth of clots in cerebral vessels, which leads to the removal of serum and liquid phase from the clot over time.

For alteplase, the complete dissolution times for coarse, fine, and retracted clots are 644, 1433, and 1584 seconds, respectively. Reteplase takes 2779, 3115, and 3634 seconds for the same clot types. Tenecteplase achieves complete dissolution in 829, 1572, and 1883 seconds, respectively. Fine clots, characterized by their packed structure and smaller pores, exhibit lower permeability, leading to longer dissolution times compared to coarse clots. Retracted clots, with reduced permeability due to serum removal, also take longer to dissolve compared to non-retracted clots. Reteplase does not show superior efficacy compared to alteplase in clinical studies [21,49], and our findings confirm a longer dissolution time for it. In contrast, tenecteplase, which has a similar dissolution time to alteplase but a lower bleeding risk, is a promising candidate for thrombolytic treatment. Several studies have demonstrated that tenecteplase outperforms alteplase in clinical trials, offering improved efficacy and recanalization rate [50,51] while also benefiting from a simple single-bolus injection process [52].

While this study presents a detailed computational analysis of clot lysis, several limitations should be addressed. First, the clot structure in the model is assumed to be homogeneous, whereas real thrombi have heterogeneous fibrin networks, varying red blood cell and platelet content, all of which can influence the lysis process. Additionally, the clot length used in the simulations is relatively short compared to the thrombus sizes observed in clinical cases, which may affect the results. Another simplification is the assumption of a constant arterial flow rate, whereas in vivo conditions involve pulsatile flow patterns that can alter drug transport. Addressing these limitations in future studies by incorporating more realistic clot heterogeneity, longer clots, and pulsatile flow conditions could further improve the accuracy and clinical relevance.

5. Conclusion

The study investigated the efficacy of three plasminogen activators—alteplase, reteplase, and tenecteplase—in dissolving clots with various structures. Clots with coarse fibrin fibers (radius of 100 nm), fine fibrin fibers (radius of 60 nm), and retracted clots (older clots with reduced liquid phase) were examined. These clots were located in the MCA after the ICA bifurcation, causing complete occlusion. Findings revealed that all three drug regimens were safe and associated with a low risk of bleeding. Alteplase, with its higher injection dose, resulted in faster clot dissolution across all structures, with blood flow restored in 10.4, 15.8, and 23.3 minutes for coarse, fine, and retracted clots, respectively. Tenecteplase, despite its lower dosage, achieved approximately similar recanalization times of 13.0, 21.3, and 26.2 minutes for the same clot types, highlighting

its potential as an alternative thrombolytic agent. Additionally, clots with a smaller fibrin radius dissolved more slowly than those with larger fibrin fibers. Retracted clots required nearly twice the time to dissolve. The key finding of this study is that while all evaluated drug dosage regimens successfully dissolved clots, lysis time is strongly influenced by both clot structure and the specific tPA variant administered. The findings provide quantitative insights into the efficacy of different tPA variants and the role of clot structure, which may aid in the selection of optimal therapeutic strategies for thrombolytic therapy. Future research can focus on exploring various drug regimens to determine the optimal dose of tenecteplase as a viable alternative to alteplase. Additionally, the presented model can be used to evaluate the efficacy of combined treatments with multiple drugs or to aid in the development of new therapeutic agents.

Conflict of interest

None.

References

[1] The top 10 causes of death. https://www.who.int/news-room/fact-sheets/detail/the-top-10-causes-of-death. Accessed: August. 7, 2024.

[2] Gabriel, D., Muga, K., and Boothroyd, E. “The effect of fibrin structure on fibrinolysis.” In: Journal of Biological Chemistry 267.34 (1992), pp. 24259–24263. DOI: 10.1016/S0021-9258(18)35759-4.

[3] Kramer, M., van der Wal, A., Koch, K., et al. “Presence of older thrombus is an independent predictor of long-term mortality in patients with ST-elevation myocardial infarction treated with thrombus aspiration during primary percutaneous coronary intervention”. In: Circulation 118.18 (2008), pp. 1810–1816. DOI:10.1161/CIRCULATIONAHA.108.780734.

[4] Holland, C., Vaidya, S., Datta, S., et al. “Ultrasound-enhanced tissue plasminogen activator thrombolysis in an in vitro porcine clot model”. In: Thrombosis research 121.5 (2008), pp. 663–673. DOI: 10.1016/j.thromres.2007.07.006.

[5] Bannish, B., Keener, J., and Fogelson, A. “Modelling fibrinolysis: a 3D stochastic multiscale model”. In: Mathematical medicine and biology: a journal of the IMA 31.1 (2014), pp. 17–44. DOI: 10.1093/imammb/dqs029.

[6] Carr, M., and Alving, B. “Effect of fibrin structure on plasmin-mediated dissolution of plasma clots”. In: Blood coagulation & fibrinolysis 6.6 (1995), pp. 567–573. DOI: 10.1097/00001721-199509000-00011.

[7] Collet, J., Soria, J., Mirshahi, M., et al. “Dusart syndrome: a new concept of the relationship between fibrin clot architecture and fibrin clot degradability: hypofibrinolysis related to an abnormal clot structure”. In: (1993). DOI: 10.1182/blood.V82.8.2462.2462.

[8] Collet, J., Lesty, C., Montalescot, G., et al. “Dynamic changes of fibrin architecture during fibrin formation and intrinsic fibrinolysis of fibrin-rich clots”. In: Journal of Biological Chemistry 278.24 (2003), pp. 21331–21335. DOI: 10.1074/jbc.M212734200.

[9] Diamond, S., and Anand, S. “Inner clot diffusion and permeation during fibrinolysis”. In: Biophysical journal 65.6 (1993), pp. 2622–2643. DOI: 10.1016/S0006-3495(93)81314-6.

[10] Kolev, K., Tenekedjiev, K., Komorowicz, E., et al. “Functional evaluation of the structural features of proteases and their substrate in fibrin surface degradation”. In: Journal of Biological Chemistry 272.21 (1997), pp. 13666–13675. DOI: 10.1074/jbc.272.21.13666.

[11] Kunitada, S., FitzGerald, G., and Fitzgerald, D. “Inhibition of clot lysis and decreased binding of tissue-type plasminogen activator as a consequence of clot retraction”. In: (1992). DOI: 10.1182/blood.V79.6.1420.1420.

[12] Fox, J., and Phillips, D. “Polymerization and organization of actin filaments within platelets”. In: Seminars in hematology. Vol. 20. 4, pp. 243–260. PMID: 6316555.1983.

[13] Sabovic, M., Lijnen, H., Keber, D., et al. “Effect of retraction on the lysis of human clots with fibrin specific and non-fibrin specific plasminogen activators”. In: Thrombosis and haemostasis 62.08 (1989), pp. 1083–1087. DOI: 10.1055/s-0038-1647122.

[14] Sabovic, M., Lijnen, H., Keber, D., et al. “Correlation between progressive adsorption of plasminogen to blood clots and their sensitivity to lysis”. In: Thrombosis and haemostasis 64.07 (1990), pp. 450–454. DOI: 10.1055/s-0038-1647335.

[15] Adivitiya., and Pal Khasa, Y. “The evolution of recombinant thrombolytics: Current status and future directions”. In: Bioengineered 8.4 (2017), pp. 331–358. DOI: 10.1080/21655979.2016.1229718.

[16] Lemmon, G. Vascular Surgery: Principles and Practice, Samuel Eric Wilson, Juan Carlos Jimenez, Frank J. Veith, A. Ross Naylor, and John AC Buckels, editors,©, CRC Press (2017), LLC ISBN-10: 1482239450; 950 pages. Cost: hardcopy, 289.95; e − book,202.97. 2018. DOI: 10.1016/j.jvs.2017.10.008.

[17] Fletcher, A., Alkjaersig, N., Lewis, M., et al. “A pilot study of urokinase therapy in cerebral infarction.” In: Stroke 7.2 (1976), pp. 135–142. DOI: 10.1161/01.STR.7.2.135.

[18] Multicenter Acute Stroke Trial. “Thrombolytic therapy with streptokinase in acute ischemic stroke”. In: The New England journal of medicine 335.3 (1996), pp. 145–150. DOI: 10.1056/NEJM199607183350301.

[19] Nikitin, D., Choi, S., Mican, J., et al. “Development and testing of thrombolytics in stroke”. In: Journal of Stroke 23.1 (2021), pp. 12–36. DOI: 10.5853/jos.2020.03349.

[20] Warach, S., Dula, A., and Milling, T. “Tenecteplase thrombolysis for acute ischemic stroke”. In: Stroke 51.11 (2020), pp. 3440–3451. DOI: 10.1161/STROKEAHA.120.029749.

[21] Simpson, D., Siddiqui, M., Scott, L., et al. “Reteplase: a review of its use in the management of thrombotic occlusive disorders”. In: American journal of cardiovascular drugs 6 (2006), pp. 265–285. DOI: 10.2165/00129784-200606040-00007.

[22] Melandri, G., Vagnarelli, F., Calabrese, D., et al. “Review of tenecteplase (TNKase) in the treatment of acute myocardial infarction”. In: Vascular health and risk management (2009), pp. 249–256. DOI: 10.2147/vhrm.s3848.

[23] Menon, B., Buck, B., Singh, N., et al. “Intravenous tenecteplase compared with alteplase for acute ischaemic stroke in Canada (AcT): a pragmatic, multicentre, open-label, registry-linked, randomised, controlled, non- inferiority trial”. In: The Lancet 400.10347 (2022), pp. 161–169. DOI: 10.1016/S0140-6736(22)01054-6.

[24] Piebalgs, A., Gu, B., Roi, D., et al. “Computational simulations of thrombolytic therapy in acute ischaemic stroke”. In: Scientific reports 8.1 (2018), p. 15810. DOI: 10.1038/s41598-018-34082-7.

[25] Gu, B., Piebalgs, A., Huang, Y., et al. “Mathematical modelling of intravenous thrombolysis in acute ischaemic stroke: Effects of dose regimens on levels of fibrinolytic proteins and clot lysis time”. In: Pharmaceutics 11.3 (2019), p. 111. DOI: 10.3390/pharmaceutics11030111.

[26] Ghasemi, S., Ahmadian, MT., and Assempour, A. “Computational modeling of blood clot lysis considering the effect of vessel wall and pulsatile blood flow”. In: Physical Review E 108.3 (2023), p. 034403. DOI: 10.1103/PhysRevE.108.034403.
[27] Yang, Y., Gu, B., and Xu, X. “In silico study of different thrombolytic agents for fibrinolysis in acute ischemic stroke”. In: Pharmaceutics 15.3 (2023), p. 797. DOI: 10.3390/pharmaceutics15030797.
[28] Yang, Y., Gu, B., and Xu, X. “In silico study of combination thrombolytic therapy with alteplase and mutant pro-urokinase for fibrinolysis in ischemic stroke”. In: Computers in Biology and Medicine 171 (2024), p. 108141. DOI: 10.1016/j.compbiomed.2024.108141.
[29] Raynaud, F., Rousseau, A., Monteyne, D., et al. “Investigating the two regimes of fibrin clot lysis: an experimental and computational approach”. In: Biophysical journal 120.18 (2021), pp. 4091–4106. DOI: 10.1016/j.bpj.2021.08.005.
[30] Gutierrez, J., Rosoklija, G., Murray, J., et al. “A quantitative perspective to the study of brain arterial remodeling of donors with and without HIV in the Brain Arterial Remodeling Study (BARS)”. In: Frontiers in physiology 5 (2014), p. 56. DOI: 10.3389/fphys.2014.00056.
[31] Nield, D., and Bejan, A. Convection in porous media. Springer, 2017. DOI: 10.1007/978-3-319-49562-0.
[32] Blanco, P., Watanabe, S., Passos, M., et al. “An anatomically detailed arterial network model for one-dimensional computational hemodynamics”. In: IEEE Transactions on biomedical engineering 62.2 (2014), pp. 736–753. DOI: 10.1109/TBME.2014.2364522.
[33] Westerhof, N., Lankhaar, J., and Westerhof, B. “The arterial windkessel”. In: Medical & biological engineering & computing 47.2 (2009), pp. 131–141. DOI: 10.1007/s11517-008-0359-2.
[34] Xiao, N., Humphrey, J., and Figueroa, C. “Multi-scale computational model of three-dimensional hemodynamics within a deformable full-body arterial network”. In: Journal of computational physics 244 (2013), pp. 22–40. DOI: 10.1016/j.jcp.2012.09.016.
[35] Sobel, B., Gross, R., and Robison, A. “Thrombolysis, clot selectivity, and kinetics.” In: Circulation 70.2 (1984), pp. 160–164. DOI: 10.1161/01.CIR.70.2.160.
[36] Collen, D., Zamarron, C., Lijnen, H., et al. “Activation of plasminogen by pro-urokinase. II. Kinetics.” In: Journal of Biological Chemistry 261.3 (1986), pp. 1259–1266. PMID: 2935529.
[37] Tiefenbrunn, A., Graor, R., Robison, A., et al. “Pharmacodynamics of tissue-type plasminogen activator characterized by computerassisted simulation.” In: Circulation 73.6 (1986), pp. 1291–1299. DOI: 10.1161/01.cir.73.6.1291.
[38] Chandler, W., Alessi, M., Aillaud, M., et al. “Clearance of tissue plasminogen activator (TPA) and TPA/plasminogen activator inhibitor type 1 (PAI-1) complex: relationship to elevated TPA antigen in patients with high PAI-1 activity levels”. In: Circulation 96.3 (1997), pp. 761–768. DOI: 10.1161/01.cir.96.3.761.
[39] Hekman, C., and Loskutoff, D. “Kinetic analysis of the interactions between plasminogen activator inhibitor 1 and both urokinase and tissue plasminogen activator”. In: Archives of biochemistry and biophysics 262.1 (1988), pp. 199–210. DOI: 10.1016/0003-9861(88)90182-8.
[40] Husain, S., Hasan, AA., and Budzynski, A. “Differences between binding of one-chain and two-chain tissue plasminogen activators to non-cross-linked and cross-linked fibrin clots”. In: Blood 74.3 (1989), pp. 999-1006. DOI: 10.1182/blood.V74.3.999.999.
[41] Wootton, D., Popel, A., and Alevriadou, B. “An experimental and theoretical study on the dissolution of mural fibrin clots by tissue-type plasminogen activator”. In: Biotechnology and bioengineering 77.4 (2002), pp. 405–419. DOI: 10.1002/bit.10127.
[42] Lucas, M., Straight, D., Fretto, L., et al. “The effects of fibrinogen and its cleavage products on the kinetics of plasminogen activation by urokinase and subsequent plasmin activity.” In: Journal of Biological Chemistry 258.20 (1983), pp. 12171–12177. DOI: 10.1016/S0021-9258(17)44152-4.
[43] Davies, C. “The separation of airborne dust and particles”. In: Proceedings of the Institution of mechanical engineers 167.1b (1953), pp. 185–213. DOI: 10.1177/002034835316701b13.
[44] Diamond, S. “Engineering design of optimal strategies for blood clot dissolution”. In: Annual review of biomedical engineering 1.1 (1999), pp. 427–461. DOI: 10.1146/annurev.bioeng.1.1.427.
[45] Schenk, O., and Gärtner, K. “Solving unsymmetric sparse systems of linear equations with PARDISO”. In: Future Generation Computer Systems 20.3 (2004), pp. 475–487. DOI: 10.1016/j.future.2003.07.011.
[46] Shaz, B., and Hillyer, C. Transfusion medicine and hemostasis: clinical and laboratory aspects. Elsevier Science, 2019. DOI: 10.1016/C2015-0-05783-5.
[47] Alexandrov, A., Burgin, W., Demchuk, A., et al. “Speed of intracranial clot lysis with intravenous tissue plasminogen activator therapy: sonographic classification and short-term improvement”. In: Circulation 103.24 (2001), pp. 2897–2902. DOI: 10.1161/01.CIR.103.24.2897.
[48] Christou, I., Alexandrov, A., Burgin, W., et al. “Timing of recanalization after tissue plasminogen activator therapy determined by transcranial Doppler correlates with clinical recovery from ischemic stroke”. In: Stroke 31.8 (2000), pp. 1812–1816. DOI: 10.1161/01.STR.31.8.1812.
[49] Lin, Z., Qiu, H., Tong, X., et al. “Evaluation of efficacy and safety of Reteplase and Alteplase in the treatment of hyper-acute cerebral infarction”. In: Bioscience Reports 38.1 (2018), BSR20170730. DOI: 10.1042/BSR20170730.
[50] Alhadid, K., Oliveira, L., and Etherton, M. “Intravenous thrombolytics in the treatment of acute ischemic stroke”. In: Current Treatment Options in Cardiovascular Medicine 25.1 (2023), pp. 15–28. DOI: 10.1007/s11936-022-00973-2.
[51] Potla, N., and Ganti, L. “Tenecteplase vs. alteplase for acute ischemic stroke: a systematic review”. In: International journal of emergency medicine 15.1 (2022), p. 1. DOI: 10.1186/s12245-021-00399-w.

[52] Zubair, A., and Sheth, K. “IV tenecteplase: A non-inferior alternative to alteplase?” In: Med 3.8 (2022), pp. 519–520. DOI: 10.1016/j.medj.2022.07.006.

Biographies

Saleheh Heydari Ghasemi received her B.Sc. degree in Mechanical Engineering from K. N. Toosi University of Technology, Tehran, Iran, in 2013, where she also completed her M.Sc. in Mechanical Engineering in 2016. Since 2018, she has been pursuing a Ph.D. in Mechanical Engineering at Sharif University of Technology. Her research interests lie in the field of bioengineering.

Mohammad Taghi Ahmadian received his BS and MS degrees in Physics in 1972 from Shiraz University, Shiraz, Iran and completed the requirements for BS and MS degrees in Mechanical Engineering in 1980 from University of Kansas in Lawrence. At the same time, while getting his master’s degree, he completed his PhD in Physics and PhD in Mechanical Engineering in 1981 and 1986, respectively, from University of Kansas. He started working as an Assistant Professor at Sharif university of Technology in 1989; at present, he is a Professor in the School of Mechanical Engineering in Sharif University of Technology, Tehran.

Ahmad Assempour received his B.Sc. and M.Sc. degrees in Mechanical Engineering (Applied Mechanics) from Tehran Polytechnic in 1979 and 1985, respectively. He earned his Ph.D. in Mechanical Engineering from Oklahoma State University in December 1989. He is currently a Professor in the School of Mechanical Engineering at Sharif University of Technology, Tehran, Iran.

Figure captions

Figure 1. Geometry of the ICA bifurcation

Figure 2. Temporal variation in the plasma concentration of a) tPA, b) uPA, c) PLG, d) FBG, e) AP, f) MG, g) PAI-1, and h) PLS after injection of alteplase (blue), reteplase (orange), and tenecteplase (green)

Figure 3. Changes in the porosity of the coarse (blue), fine (orange), and retracted (green) clots after administration of a) alteplase, b) reteplase, and c) tenecteplase

Figure 4. Recanalization time for the different drugs and clot structures

Table captions

Table 1. Reactions performed in plasma

Table 2. Reactions performed in the clot

Table 3. Description of the different drugs and clot structures in the simulations

Table 1:

No.	Re*actions*	Re *ference*
1	$tPA + PLG \xrightarrow{K_{1,M}, k_{1,cat}} tPA + PLS$	[35]
2	$uPA + PLG \xrightarrow{K_{4,M}, k_{4,cat}} uPA + PLS$	[36]
3	$PLS + AP \underset{k_{2,r}}{\overset{k_{2,f}}{\rightleftarrows}} PLS.AP \xrightarrow{k2.cat} inactive$	[35]
4	$PLS + FBG \xrightarrow{K_{3,M}, k_{3,cat}} PLS + FDP$	[35]
5	$PLS + MG \xrightarrow{k_4} inactive$	[37]
6	$tPA + PAI \xrightarrow{k_5} inactive$	[38]
7	$uPA + PAI \xrightarrow{k_6} inactive$	[39]

Table 2:

No.	Re*actions*	Re *ference*
1	$tPA + fibrin \underset{k_{d,tPA}}{\overset{k_{a,tPA}}{\rightleftarrows}} tPA \cdot fibrin$	[40]
2	$PLG + fibrin \underset{k_{d,PLG}}{\overset{k_{a,PLG}}{\rightleftarrows}} PLG \cdot fibrin$	[41]
3	$PLS + fibrin \underset{k_{d,PLS}}{\overset{k_{a,PLS}}{\rightleftarrows}} PLS \cdot fibrin$	[41]
4	$tPA \cdot fibrin + PLG \cdot fibrin \xrightarrow{K_M, k_{M,cat}} tPA \cdot fibrin + PLS \cdot fibrin$	[25]
5	$uPA + PLG \cdot fibrin \xrightarrow{K_{M,uPA}, k_{cat,uPA}} uPA + PLS \cdot fibrin$	[42]
6	$PLS \cdot fibrin \xrightarrow{k_{deg}} PLS + FDP$	[11]

Table 3:

No.	*Drug used*	*Clot type*	*Fiber radius* (*nm*)
1	*Alteplase*	*Non* – Re*tracted*	100
2	*Alteplase*	*Non* – Re*tracted*	60
3	*Alteplase*	Re*tracted*	100
4	Re*teplase*	*Non* – Re*tracted*	100
5	Re*teplase*	*Non* – Re*tracted*	60
6	Re*teplase*	Re*tracted*	100
7	*Tenecteplase*	*Non* – Re*tracted*	100
8	*Tenecteplase*	*Non* – Re*tracted*	60
9	*Tenecteplase*	Re*tracted*	100

Figure 1:

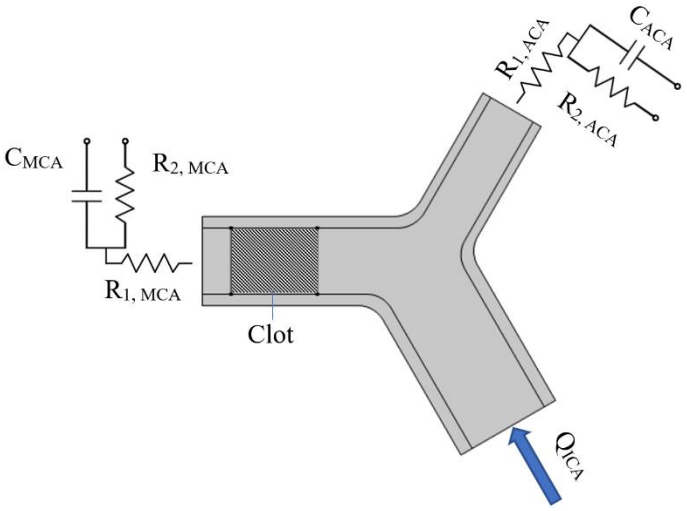

Figure 2:

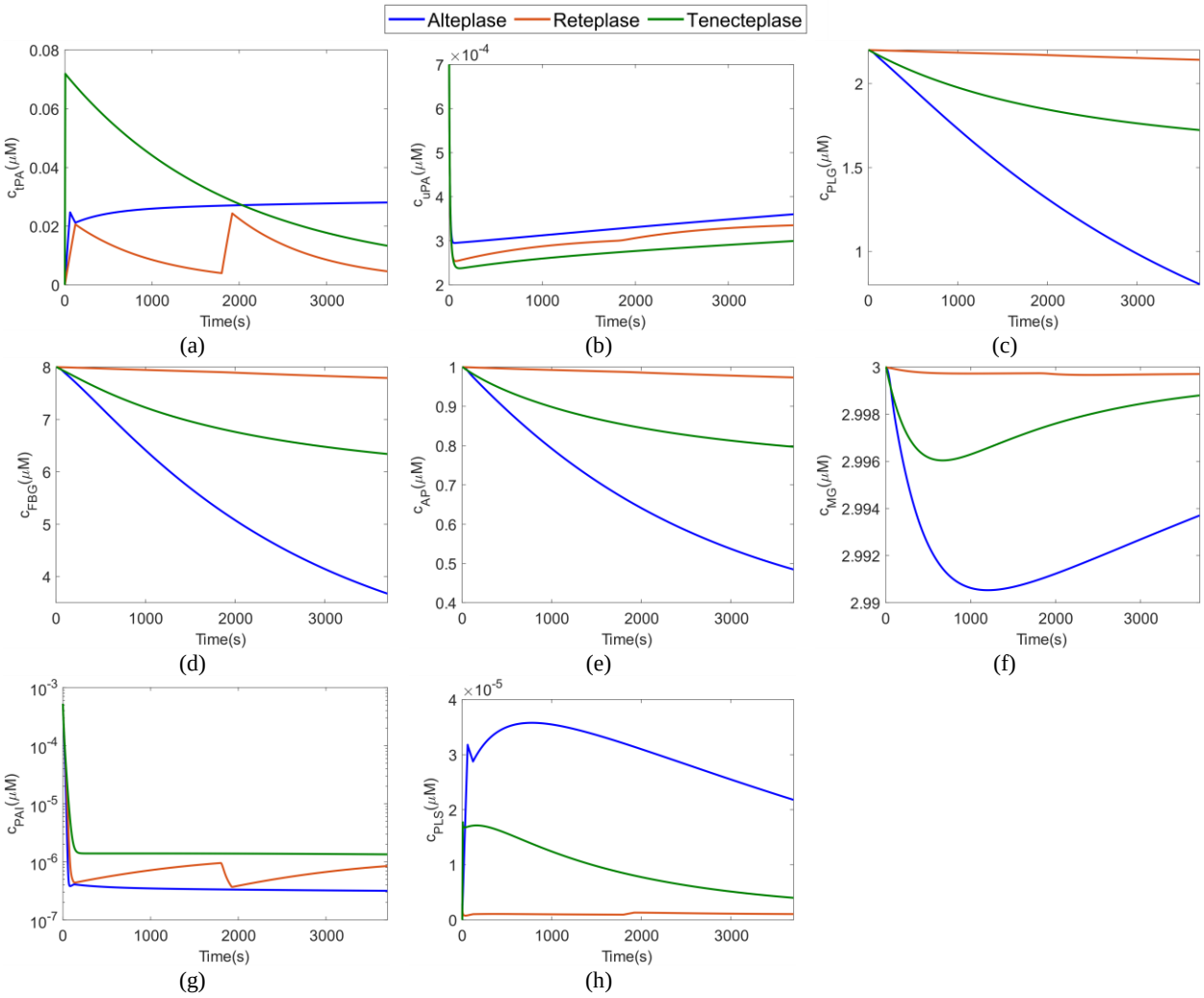
Alteplase
Reteplase
Tenecteplase
$c_{tPA}(\mu M)$
$c_{uPA}(\mu M)$
$c_{PLG}(\mu M)$
$c_{FBG}(\mu M)$
$c_{AP}(\mu M)$
$c_{MG}(\mu M)$
$c_{PAI}(\mu M)$
$c_{PLS}(\mu M)$
Time(s)
(a)
(b)
(c)
(d)
(e)
(f)
(g)
(h)

Figure 3:

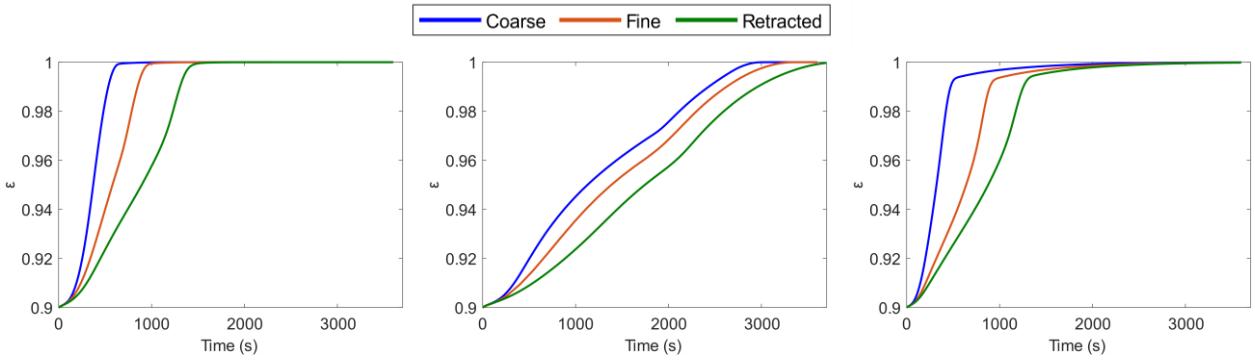
Coarse
Fine
Retracted
1
0.98
0.96
0.94
0.92
0.9
3
0
1000
2000
3000
Time (s)

(a) (b) (c)

Figure 4:

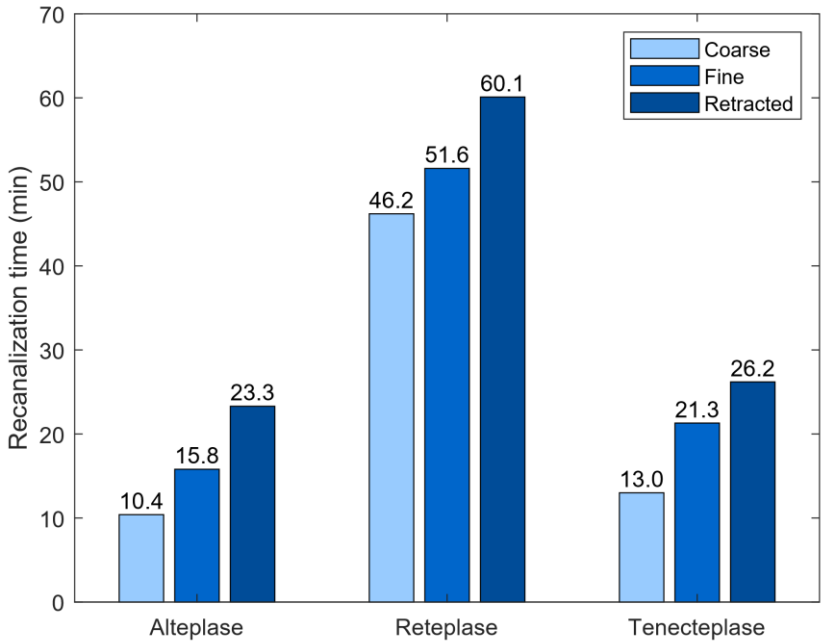
Recanalization time (min)
0
10
20
30
40
50
60
70
Coarse
Fine
Retracted
10.4
15.8
23.3
46.2
51.6
60.1
13.0
21.3
26.2
Alteplase
Reteplase
Tenecteplase